

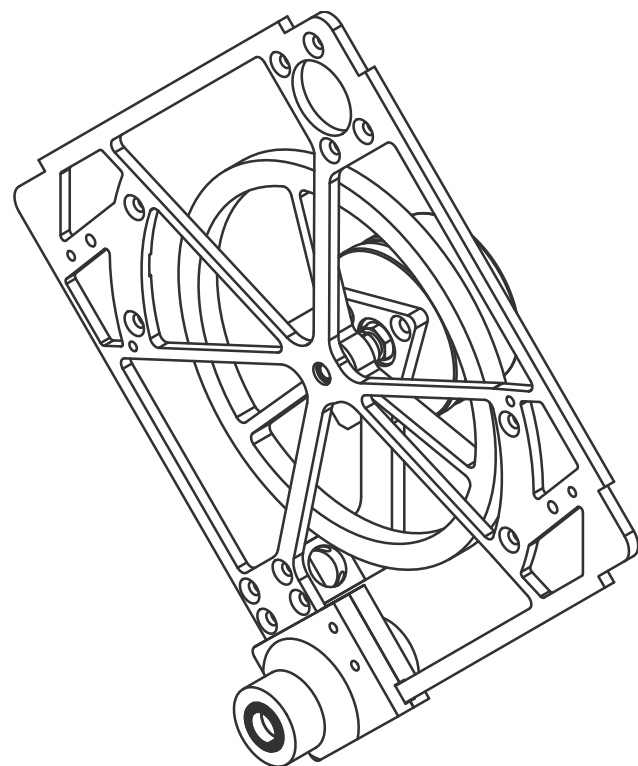
# Linear Quadratic Regulation of Reaction Wheel Stabilised Pendulum

Semesterarbeit von

Kyle Kenney

Am Fachbereich 15  
Fachgebiet Elektrische Maschinen und Antriebe

Fachgebietsleiter: Prof. Dr.-Ing. M.Ziegler  
Betreuer: Dipl.-Ing. Lars Tabit



Kyle Kenney  
Liebig str 6  
34125 Kassel geb.: 23.12.1986, Nova Scotia, Kanada  
Matr.-Nr.: 32202601

**Eigenstaendigkeitserklaerung**

Ich erklaere hiermit, die vorliegende Arbeit selbststaendig verfasst zu haben. Es wurden keine unerlaubten Hilfsmittel und nur die im Literaturverzeichnis angegebenen Quellen verwendet. Ich versichere, keine unzulaessige fremde Hilfe in Anspruch genommen zu haben.

Kassel, den 29.9.20

---

# Index

<b>1 All Models are wrong</b>	<b>7</b>
1.1 The (Not So) Simple Pendulum . . . . .	7
1.2 Back to Basics: Part <i>I</i> . . . . .	8
1.2.1 The Lagrangian Equations . . . . .	9
1.2.2 Potential and Kinetic Energy . . . . .	10
1.2.3 The Lagrangian . . . . .	11
1.3 The State Space Model . . . . .	12
1.3.1 Linearisation in StateSpace . . . . .	12
1.4 Conclusion . . . . .	13
<b>2 Prototype</b>	<b>14</b>
2.1 The McGuffin, history and other things. . . . .	14
2.2 Electrical Design . . . . .	15
2.3 Mechanical Design . . . . .	15
<b>3 Parameter Identification</b>	<b>17</b>
3.1 Parameters to identify . . . . .	17
3.2 IMU Calibration . . . . .	17
3.2.1 Accelerometer and Gyroscope . . . . .	18
3.2.2 Magnetometer . . . . .	18
3.3 Madgwick Filter . . . . .	19
3.4 Centre of Mass Approximation . . . . .	20
3.5 This one goes up to 11 . . . . .	21
3.5.1 Nonlinear Identification . . . . .	21
3.5.2 Flywheel Moment of Inertia, Friction Coefficient . . . . .	21
3.5.3 Fullbody Moment of Inertia, Friction Coefficient . . . . .	23
3.6 Conclusion . . . . .	25
<b>4 Controller Design</b>	<b>26</b>
4.1 Back to Basics: Part <i>Deux</i> . . . . .	26
4.1.1 Analysis . . . . .	27
4.2 Linear Quadratic Regulator . . . . .	28
4.2.1 Conclusion . . . . .	30
<b>5 Implementation and Results</b>	<b>31</b>
5.1 Results and Comparison . . . . .	32
5.2 Conclusion and Future Work . . . . .	33

# Nomenclature

## Greek Symbols

Symbol	Description	Dimensions	Units
$\alpha$	Fly Wheel Body Angle	$rad$	$c$
$\ddot{\varphi}$	Pendulum Body Angular Acceleration	$radS$	$c\ s^{-2}$
$\dot{\alpha}$	Pendulum Body Angular Velocity	$radS$	$c\ s^{-1}$
$\dot{\varphi}$	Fly Wheel Angular Velocity	$radS$	$c\ s^{-1}$
$\iota$	Friction Coefficient	—	—
$\mu$	Friction Coefficient	—	—
$\Omega$	Ohm	$ML^2 A^{-2} S^{-3}$	$\frac{kgm^2}{A^2 s^3}$
$\pi$	Apple	$rad$	$c$
$\tau$	Torque Constant	$MA^{-1} L^2 S^6$	$m\ N\ m\ A^{-1}$
$\Theta$	Total Moment of Inertia	$ML^2$	$kg\ m^2$
$\varphi$	Pendulum Body Angle	$rad$	$c$
$O$	Omicron Persi 8	$ML^3$	$kg\ m^3\ 2^3$

## Roman Symbols

Symbol	Description	Dimensions	Units
$e$	Euler Constant	—	—
$f_x$	Input Force X Component	$MKS^2$	$kg\ m\ s^2$
$f_y$	Input Force Y Component	$MKS^2$	$kg\ m\ s^2$
$g$	Gravitational Constant On Earth Surface	$MS^{-2}$	$ms^{-2}$
$j_b$	Pendulum Body Moment of Inertia	$ML^2$	$kg\ m^2$
$j_w$	Flywheel Moment of Inertia	$ML^2$	$kg\ m^2$
$k$	Centre of Fly Wheel Rotation	$L$	$m$
$k_i$	Regulator Coefficient	—	—
$l$	Centre of Mass	$L$	$m$

$m_b$	Pendulum Body Mass	$M$	kg
$m_w$	Flywheel Mass	$M$	kg
$r_b$	Friction Coefficient	-	-
$r_w$	Friction Coefficient	-	-
$s$	Centre of Inertia Motion Unit	$L$	m
$X_i$	Coordinate labels	-	-
$z$	Frequency	$S^{-1}$	$s^{-1}$

## Other Symbols

Symbol	Description	Dimensions	Units
$\mathbb{C}$	Complex Numbers	-	-
$\mathbb{H}$	Quaternions Numbers	-	-
$\mathbb{I}$	Irrational Numbers	-	-
$\mathbb{N}$	Natural Numbers	-	-
$\mathbb{Q}$	Rational Numbers	-	-
$\mathbb{R}$	Real Numbers	-	-
$\mathbb{Z}$	Integer Numbers	-	-
$\mathcal{L}$	Laplace Operator	-	-

# Intro

Those who love Analysis will see with pleasure that Mechanics has become a branch of it, and will be grateful to me for having thus extended its domain.

---

Joseph-Louis Lagrange

Todays world is completely governed by automation, the food we eat, the machines we drive, the power we use every day has some form or another of an automaton behind it. These machines are also becoming more intelligent. It is completely common to find even vacuums with sophisticated learning and control techniques inside of them.

The lowly robot vacuum, though, may even become the ancient ancestor of an entirely new form of intelligence in the future, and one that may wonder how such prehistoric creatures could have even lived, much like how humanity ponders its earlier prehistoric relatives' existence. Though this may just be something from the author's fantasy, it isn't even a new idea. It seems humanity has desired to create artificial life of its own for quite a long time. When looking back in history at automation most will probably think Ford was the first to automate industrial processes. Or the Japanese in the 1930s. [1]. However, it is often forgotten that the first lathe, arguably the first tool of automated work, was already in use circa 1750. [2]

One could also forgive those not well read for thinking that the first ideas of automation must have started then. However this is certainly wrong. Even the Greeks, between 200 and 70 B.C., actually *built* machines for automation. The *Antikythera Mechanismus*, a mechanical analogue computer was built with complicated inner workings to calculate and predict the elliptical orbits of astronomical bodies years ahead of time.[3]

But in fact even this isn't the first ever concept of automation. Homer already in the year 800 B.C. sought to have machines walking around. Twenty 'Automatons' were built by *Hephaestus* to serve the gods.[3]

It is quite apparent that humanity has always wanted to have machines and robots around. It is, however, only within the last decades that society has gained the technical know-how and the computer power to really put forth the ideas Homer had so many centuries ago. In order to start to grasp at the ideas of some kind of future intelligence however, one must first start with the basics.

The lowest form of machine with a questionable definition of intelligence, the inverted simple pendulum, must be given life, investigated, understood and controlled. Without fully grasping the basics, the greeks automatons will remain the realm of just science fiction.

# Chapter 1

## All Models are wrong

Remember that all models are wrong; the practical question is how wrong do they have to be to not be useful."

---

George Box

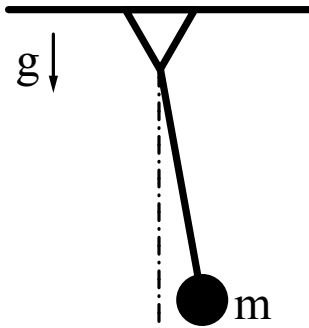


Figure 1.1: The Simple Pendulum

### 1.1 The (Not So) Simple Pendulum

The Simple Pendulum, a relatively simple mechanical system requiring little more beyond a bit of string and a any sort of easily tie-able object. This system can be easily put into a planar oscillating motion by simply pulling up, letting go and letting gravity do the rest of the work. So intuitive is its motion that any child with some courage in their pocket and a few minutes around the play-ground swing can master its motion.

Unfortunately, nothing in life is ever as simple as the play-ground swing. Much as the difficulty of swinging higher on a swing increases once a person gets close to horizontal, the pendulum hides within its kinematics a not so obvious surprise of complexity. Counter to intuition of one's 'feeling', the mass of a swinging weight plays no important, or in fact, any role at all in its sweep. The motion of the simple pendulum is also nonlinear.[4]

$$\ddot{\varphi} + \frac{g}{l} \sin \varphi = 0 \quad (1.1)$$

This nonlinearity leads to hard to solve ordinary differential equations of second order requiring the execution of difficult maths, or numerical solutions and algorithms to describe its exact motion. What may also come as a surprise to almost no one who has ever tried to balance a metre stick on their finger, the pendulum has exactly two stable stationary points, using a generalised form of Equation 1.1

$$\ddot{x}(t) + a \sin(x(t)) = 0$$

the second derivative of

$$\ddot{x}(t) = 0$$

exactly when

$$x(t) = c$$

as such 1.1 can be solved as

$$n \in \mathbb{Z} \wedge x(t) = 2\pi n \vee x(t) = 2\pi n + \pi \vee a = 0$$

Or to be slightly less exact but more clear,

$$x(t) = \pi n, n \in \mathbb{Z}$$

Leaving the simple pendulum a fairly boring absolutely stable stationary system when  $x(t) = 2n\pi$  and the far more interesting marginally stable stationary point when  $x(t) \equiv \pi$  or any  $2n - 1$  multitude of it. The marginal stability of the inverted pendulum lends itself as the ideal candidate for applying controlling techniques to reduce the system to a globally stable one. Further analysis, system derivation and controller development will be on the inverted pendulum.

However any child with a long enough stick and a finger could have pointed out that a pendulum will *only* stand motionless under its own accord when vertically aligned with gravity, while at the same time putting money where their mouth is, balancing the stick effortlessly, motionless on said finger. They will neglect to mention the countless hours spent learning how to perfectly match the reactionary movements of their hand to the unstable falling of the pendulum. Unfortunately the labours and time of young youth isn't the same as when one is fully adult. To solve the mechanical problems we must relinquish ourselves to the rigours of calculus to come to the same solution. But this is surely entertaining in its own way.

## 1.2 Back to Basics: Part I

The Flywheel Pendulum is a simple modification to the classical Inverted pendulum [5]. Used as an excellent source for teaching, the Flywheel pendulum is a mechanically simple, nonlinear and underactuated robotic platform[6]. Its basic but complicated dynamics make the flywheel pendulum an excellent benchmarking tool and testbench for practical applications of many multitudes of engineering.

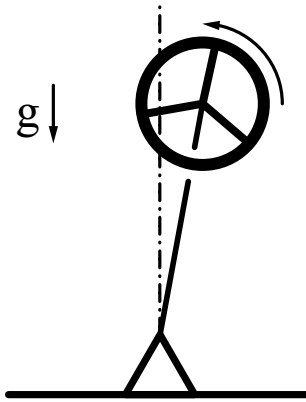


Figure 1.2: Flywheel Inverse Pendulum

In order to derive our pendulums equation of motion, a first attempt to break down it down to individual acting forces must be done. Common in mechanical analysis, Newtons method, free body analysis can be implemented.[7] Newton's second law of motion in each coordinate axis,

Summing all found forces and moments

$$\sum_{i=1}^n F_i = 0 \text{ and } \sum_{i=1}^m M_i = 0$$

will produce a cacophony of equations and variables surely to overwhelm even the soundest of minds leading to error and lost time. To avoid such a particular onslaught of mathematics, there are other methods to consider when looking into the dynamics for most any mechanical system, Trading 'simple' visual analyses and rigorous arithmetic for an almost recipe form of mathematical complexity.

### 1.2.1 The Lagrangian Equations

To derive the systems equations of motions the Euler-Lagrange Differential Equations developed by Joseph-Louis Lagrange [8] of the second form will be used. These equations state that if  $J$  is defined by an integral of the form:

$$J = \int L(t, y, \dot{y}) dt$$

where

$$\dot{y} \equiv \frac{dy}{dt}$$

Replacing the time derivative of  $\dot{y}$  with general coordinates space derivative  $q_i$  the Euler-Lagrange equation becomes [9]

$$\frac{\partial L}{\partial q_i} - \frac{d}{dt} \left( \frac{\partial L}{\partial \dot{q}_i} \right) = Q_i \quad (1.2)$$

with generalised forces  $Q_i$

The Lagrange Function  $L(t, q, \dot{q})$  described as the summation of kinetic energy subtracting the potential

$$L = T - V \quad (1.3)$$

will be built following a strict method of analyses of figure 1.3

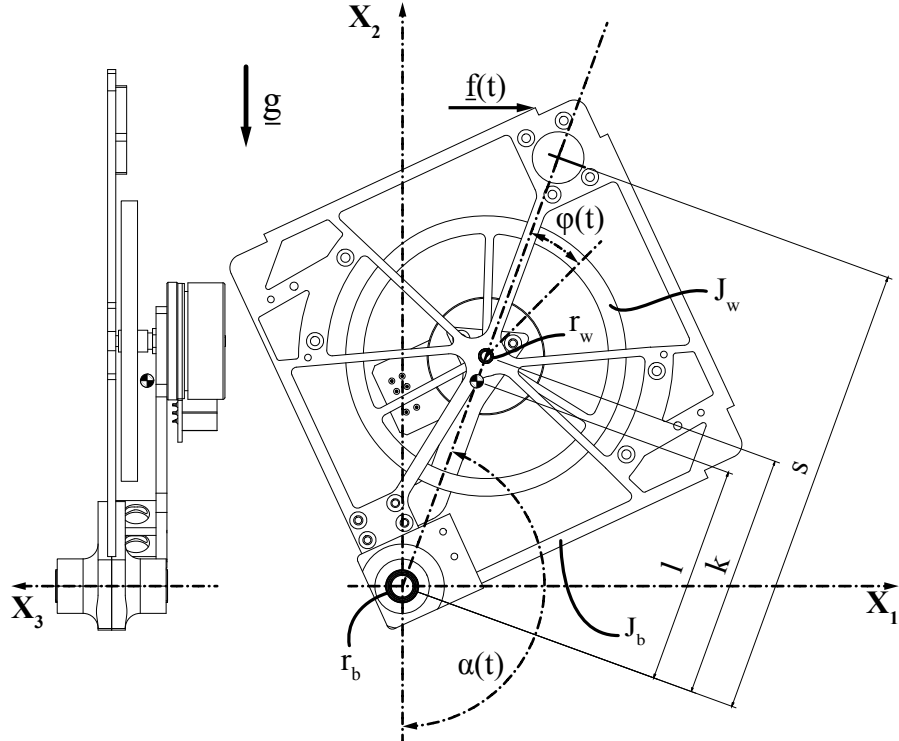


Figure 1.3: Flywheel Inverse Pendulum Schematic

### 1.2.2 Potential and Kinetic Energy

The centre of mass and motor axis as body particles in planar mechanics can be described easily with the  $X_1$  and  $X_2$  coordinates combined with the independent rotation of the motor  $\varphi(t)$  and  $\alpha$  giving a total of 2 translation and 2 rotational degrees of freedom, the Lagrange equations require the reduction to as few generalised coordinates as possible. As such coordinates  $X_1$  and  $X_2$  follow the centre of motion on a fixed radius which can be described equivalently through the transformation:

$$\underline{v} = \underline{e}_1 X_1 \sin(\alpha) + \underline{e}_2 X_2 \cos(\alpha) \quad (1.4)$$

Using the generalised coordinate of  $\varphi$  describing the C.O.M. of the entire body  $\underline{r}$

$$\underline{r} = \begin{pmatrix} X_1 \sin \alpha \\ -X_2 \cos \alpha \end{pmatrix} \quad (1.5)$$

to reduce equation complexity later the absolute length of  $r$  is calculated as follows

$$l = \sqrt{X_1^2 + X_2^2} \quad (1.6)$$

and substituting in 1.5 giving

$$\underline{r} = \begin{pmatrix} l \sin \alpha \\ -l \cos \alpha \end{pmatrix} \quad (1.7)$$

and the motor axis piercing-point:

$$\underline{s} = \begin{pmatrix} k \sin \alpha \\ -k \cos \alpha \end{pmatrix} \quad (1.8)$$

The total kinetic energy is the summation of translation and rotational dependent individual energy sources of the system

$$T = \sum_{i=1}^n m_i \frac{1}{2} \dot{v}_i^2 + \Theta_i \frac{1}{2} \omega_i^2 \quad (1.9)$$

Substituting 1.7 and 1.8 in 1.9 giving the total kinetic energy of

$$\frac{1}{2} j_b \dot{\alpha}^2 + \frac{1}{2} j_w (\dot{\alpha} + \dot{\phi})^2 + \frac{1}{2} m_w (k^2 \dot{\alpha}^2 \sin(\alpha)^2 + k^2 \dot{\alpha}^2 \cos(\alpha)^2) + \frac{1}{2} m_b (l^2 \dot{\alpha}^2 \sin(\alpha)^2 + l^2 \dot{\alpha}^2 \cos(\alpha)^2) \quad (1.10)$$

Simplifying to

$$T = \frac{1}{2} (\Theta \dot{\alpha}^2 + 2j_w \dot{\alpha} \dot{\phi} + j_w \dot{\phi}^2) \quad (1.11)$$

Whereby  $\Theta = (j_b + j_w + k^2 m_w + l^2 m_b)$  as the total moment of inertia.

The potential energy of the system  $V$  can be read from second component of  $\underline{r}$  and  $\underline{s}$  multiplied with their respective masses and gravity acceleration

$$V = \sum_{i=1}^n m_i g \underline{v}_{i2} = m_b g r_2 + m_w g s_2 = -(m_b g l \cos(\alpha) + m_w g k \cos(\alpha)) \quad (1.12)$$

Simplifying to

$$V = -g(k m_w + l m_b) \cos(\alpha) \quad (1.13)$$

combining the final results of 1.11 and 1.13 into equation 1.3 the final Lagrangian equation becomes

$$L = T - V = \frac{1}{2} (2g(k m_w + l m_b) \cos(\alpha) + \Theta \dot{\alpha}^2 + 2j_w \dot{\alpha} \dot{\phi} + j_w \dot{\phi}^2) \quad (1.14)$$

### 1.2.3 The Lagrangian

As there are two fully reduced generalised coordinates  $\varphi$  and  $\alpha$  there will be a total of two coupled ordinary differential equations to describe the flywheels motion. To calculate are four partial derivatives dependent on  $\varphi, \dot{\varphi}, \alpha$  and  $\dot{\alpha}$  respectively. Starting with

$$\frac{\partial L}{\partial \alpha} - \frac{d}{dt} \left( \frac{\partial L}{\partial \dot{\alpha}} \right) = 0 \quad (1.15)$$

providing

$$\frac{\partial L}{\partial \alpha} = -g(km_w + lm_b) \sin(\alpha) \quad (1.16)$$

and

$$\frac{d}{dt} \left( \frac{\partial L}{\partial \dot{\alpha}} \right) = \Theta \ddot{\alpha} + j_w \ddot{\varphi} \quad (1.17)$$

Taking the second and third partial derivatives of

$$\frac{\partial L}{\partial \varphi} - \frac{d}{dt} \left( \frac{\partial L}{\partial \dot{\varphi}} \right) = 0 \quad (1.18)$$

produces

$$\frac{d}{dt} \left( \frac{\partial L}{\partial \dot{\varphi}} \right) = 0 \quad (1.19)$$

and

$$\frac{d}{dt} \left( \frac{\partial L}{\partial \dot{\varphi}} \right) = j_w (\ddot{\alpha} + \ddot{\varphi}) \quad (1.20)$$

substituting the results of 1.16-1.20 into 1.15 and 1.18 respectively produces the left side solution:

$$\begin{aligned} \Theta \ddot{\alpha} + j_w \ddot{\varphi} + g(km_w + lm_b) \sin \alpha &= 0 \\ j_w (\ddot{\alpha} + \ddot{\varphi}) &= 0 \end{aligned} \quad (1.21)$$

The right side of the Euler-Lagrange equations, namely  $Q_i$  are the generalised forces  $i$  of general coordinates  $q_i$ . These include any dissipation forces, motor input torque  $\tau$  and disturbances  $f(t)$ .

$$\begin{aligned} Q_1 &= f_i \\ Q_2 &= \tau u(t) \end{aligned} \quad (1.22)$$

When considering the generalised forces  $Q_i$  they can be extended to include the Rayleigh Dissipation function  $R$  [10] when considering single degree of freedom ODE.

$$R = \frac{1}{2} \sum_i -r_i \dot{q}_i^2 \quad (1.23)$$

extending

$$Q_i = -\frac{\partial R_i}{\partial \dot{q}_i} + Q_i^{(nc)} \quad (1.24)$$

The Rayleigh functions described as

$$\begin{aligned} R_1 &= \frac{-r_b}{2} \dot{\alpha}_i^2 \\ R_2 &= \frac{-r_w}{2} \dot{\varphi}_i^2 \end{aligned} \quad (1.25)$$

Where as  $Q_i^{(nc)}$  represents forces not described within the Rayleigh dissipation function. Once substituting equations 1.22 and 1.25 recombining into 1.21 the final system of motion equations become

$$\begin{aligned} \Theta \ddot{\alpha} + j_w \ddot{\varphi} + r_b \dot{\alpha} + g(km_w + lm_b) \sin \alpha &= f(t) \\ j_w (\ddot{\alpha} + \ddot{\varphi}) + r_w \dot{\varphi} &= \tau u(t) \end{aligned} \quad (1.26)$$

### 1.3 The State Space Model

The system equations described in equations 1.26 are two coupled second order differential equations. with the initial conditions of  $\alpha(0) = \pi$ ,  $\dot{\alpha}(0) = 0$  and  $\dot{\varphi}(0) = 0$  the system can be represented in a non-linear system state space model.

Transforming equations 1.26 to highest order

$$\begin{aligned}\ddot{\alpha} &= -\frac{-f(t) + gkm_w \sin(\alpha) + glm_b \sin(\alpha) + r_b \dot{\alpha} + r_w \dot{\varphi} - \tau u(t)}{\Theta + j_w} \\ \ddot{\varphi} &= -\frac{j_w f(t) - gj_w km_w \sin(\alpha) - gj_w lm_b \sin(\alpha) - j_w r_b \dot{\alpha} + \Theta r_w \dot{\varphi} - \Theta \tau u(t)}{j_w (\Theta + j_w)}\end{aligned}\quad (1.27)$$

Let  $\alpha$  be equal to the state variable  $x_1$  and  $x_3$  representing  $\dot{\varphi}$ , where  $\dot{x}_1 = x_2$  the equations of motions can be rewritten in "matrix" nonlinear form:

$$\left( \begin{array}{c|c} (x_1, \pi) & x_2 \\ (x_2, 0) & -\frac{-\tau u + g \sin(x_1)(km_w + lm_b) + r_b x_2 + r_w x_3}{\Theta + j_w} \\ (x_3, 0) & \frac{\Theta \tau u + gj_w \sin(x_1)(km_w + lm_b) + j_w r_b x_2 - \Theta r_w x_3}{j_w (\Theta + j_w)} \\ \hline & \begin{array}{c} x_1 \\ x_2 \\ x_3 \end{array} \end{array} \right) \boxed{N} \quad (1.28)$$

#### 1.3.1 Linearisation in StateSpace

While the flywheel pendulum is a relatively complicated nonlinear system, it can be approximated using the Taylor Series. When considering a function  $f(t)$  the function can be equated, or near equated to a sum of the partial derivatives evaluated at any initial condition,  $x_0$  of said function ad infinitum. [11]

To consider an example of the lowly simple pendulum equation 1.1:

$$\ddot{\varphi} = -\frac{g}{l} \sin(\varphi)$$

The Taylor series will be expanded and evaluated around the expansion point  $\varphi(0) = 0 = \varphi_{e.p.}$  giving

$$f(\varphi) \approx f(\varphi_{e.p.}) + \frac{\partial f}{\partial \varphi} \Big|_{\varphi_{e.p.}} (\varphi - \varphi_0) + \frac{\partial^2 f}{\partial \varphi^2} \Big|_{\varphi_{e.p.}} (\varphi - \varphi_0) + \text{Terms of Higher Order}$$

Which when evaluated and dropping terms above the first order will provide the reduced order approximated solution

$$\ddot{\varphi} = -\frac{g}{l} \varphi$$

Though considered an impossibility leading to Zeno's Paradox of never being able to finish something without getting half of it done first, the usefulness of the particular thought experiment may be less than helpful. The Taylor series however allows a drastic reduction in system complexity sacrificing only some precision in system solution around a particular operating point.

To extend the usefulness of the Taylor series, the equations 1.28 can be rewritten in as a linear time invariant state space matrix.

$$\begin{aligned}\dot{\underline{x}} &= \underline{\underline{A}} \underline{x} + \underline{\underline{B}} \underline{u} \\ \underline{y} &= \underline{\underline{C}} \underline{x} + \underline{\underline{D}} \underline{u}\end{aligned}$$

Where

$$\underline{\underline{A}} = \begin{bmatrix} \frac{\partial f_1}{\partial x_1} & \frac{\partial f_1}{\partial x_2} & \cdots \\ \vdots & \ddots & \\ \frac{\partial f_n}{\partial x_1} & & \frac{\partial f_n}{\partial x_n} \end{bmatrix} \underline{\underline{B}} = \begin{bmatrix} \frac{\partial f_1}{\partial x_1} \\ \vdots \\ \frac{\partial f_n}{\partial x_n} \end{bmatrix} \underline{\underline{C}} = (x_1 e_1 + \cdots + x_n e_n) \quad \underline{\underline{D}} = \underline{\underline{0}}$$

Solving each first order partial derivative of the matrices  $\underline{\underline{A}}$  through  $\underline{\underline{C}}$  around the operating point  $\alpha = \pi$  results in the final linearised state space matrix:

$$\left( \begin{array}{c|ccc|c} & & & & u \\ \hline x_1 & 0 & 1 & 0 & 0 \\ x_2 & \frac{g(km_w + lm_w)}{\Theta + j_w} & -\frac{r_b}{\Theta + j_w} & -\frac{r_w}{\Theta + j_w} & \frac{\tau}{\Theta + j_w} \\ x_3 & -\frac{g(km_w + lm_w)}{\Theta + j_w} & \frac{r_b}{\Theta + j_w} & -\frac{\Theta r_w}{j_w^2 + \Theta j_w} & \frac{\Theta \tau}{j_w^2 + \Theta j_w} \\ \hline x_1 & 1 & 0 & 0 & 0 \\ x_2 & 0 & 1 & 0 & 0 \\ x_3 & 0 & 0 & 1 & 0 \end{array} \right) \boxed{S} \quad (1.29)$$

## 1.4 Conclusion

The modelling and dynamics of any mechanical system becomes a labour of love. Even the most basic of mechanical systems that we as children inherently learned out of passion or just pure determination end up displaying a surprising form of complexity when trying to model them. These systems are often enough far too complex to allow any sort of analytical solution requiring numerical methods. To avoid such work, tools such as the Taylor series and use of modern computing power can be put into use, allowing quick visual and mathematical analysis with well known methods and tools.

# Chapter 2

## Prototype

"Imitation is the sincerest form of flattery  
that mediocrity can pay to greatness"

---

Oscar Wilde

### 2.1 The McGuffin, history and other things.

The flywheel pendulum is nothing particularly new: one of the first introduced flywheel reaction pendulums was devised by Mark W. Spong, Peter Corke and Rogelio Lozano and presented in their paper "Nonlinear Control of the Inertia Wheel Pendulum" in 1999. They have been copied and used in multiple papers and projects. Of particular note for the use of flywheels in robotics are satellites. The 'SMEX Reaction/Momentum Wheel', was developed and put into use for the Small Explorer program (SMEX). A mechanism was required that could accelerate quickly, build and store energy to compensate and control the SMEX's angular momentum. [12]

Another fascinating example of the use of reaction wheels within robotics is the "Cubli" developed and designed by Mohanarajah Gajamohan, Raffaello D'Andrea and Igor Thommen. A small  $15cm^3$  cube frame with three reactions wheels. The Cubli can balance on it's edges as a single degree of freedom inverted pendulum or as a 3 dimensional inverted pendulum on its corner. [13] Much like the active control systems in some satellites the Cubli uses the reaction wheels angular momentum to stabilise the robot against disturbances and stand on its unstable equilibrium.

This particular semester work is heavily inspired by the Cubli test bench platform and takes some direct cues in the design form factor. The models size and use of a single flywheel, motor and controller type have been included within this work. The other design considerations and conclusions are discussed below.

The Flywheel inverted pendulum is therefore an initial single degree of freedom prototype and proof of concept device to be used for further study and use by students. The Pendulum is so designed that all parts can be easily swapped or exchanged with newer designs or concepts. The microcontrollers and sensors are based around inexpensive open source technologies following the Wiring programming language. Though the BLDC motor and drivers are in contrast proprietary technologies developed by maxon motors ®, they are nonetheless easily purchasable off the shelf products.

## 2.2 Electrical Design

To build and control the flywheel pendulum project low cost and availability of electronics were a high priority. The controller hardware should be readily available, accessible to non-programmers and easily swapped with newer models without having to heavily rewrite code. To fill these requirements, the ESP32 Arduino compatible microcontroller was chosen to fill the role. The esp32 feather microcontroller from Adafruit was purchased with a 240Mhz dual core ESP architecture chip.

For detecting and calculating the pendulum orientation, the FXOS8700 and FXAS21002 9 degree of freedom MARG was purchased, again from Adafruit. This breakout board has one of the lowest zero-rate levels of many gyroscopes exhibiting a drift of less than 1 degree per second.[14] Sensing of the motor angular velocity was done with an external Analog digital converter ADS1015 from Texas Instruments. The chip provides 12bit precision up to 3.3khz sampling rate. When considering the maximum revolutions of the flywheels motor range from -700 to 700  $\text{rad s}^{-1}$  and an output PWM encoder voltage range of 0-3.3V the linear function of change being  $\omega(V) = 0.00235714 \times V_{adc}$  with a detectable change in the  $V_{adc}$  voltage being  $\frac{1}{2^{12}V} = 0.000244141V$  the sensor is nearly 10 times more accurate than required.

The motor and driver purchased for the project was the maxon motor's EC45 flat and Escon 24/2 servo controller. The EC45 exhibiting a nominally large torque constant and high RPM range from 0-700  $\text{rads}^{-1}$  for it's small diametre of only 43mm. [15]

The escon 24/2 converter was choosen for it's low cost and easy control and programmability using the Escon Studio software ®. The escon allows current and speed control of the motor, including it's own built in PI controller for both modes, running at 10khz, appropriately allowing the discretisation of the motor's dynamics to be considered continuous for this devices setup. [16] The Escon servo controller allows for easy programming of it's I/O pins giving way for reading of the EC45's built in hallsensors, winding temperatures and simple control via PWM signals from the controller and vice-versa.

## 2.3 Mechanical Design

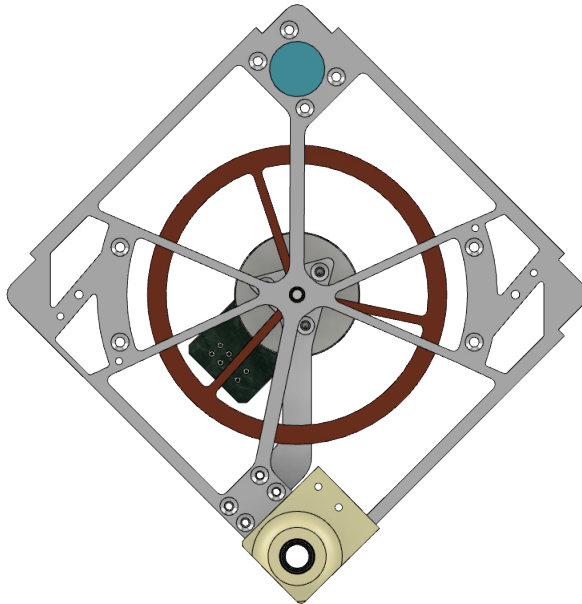


Figure 2.1: Flywheel Inverse Pendulum Render

Several constraints were required to design the F.P. The frame should be  $15\text{cm}^2$  with low moment of inertia and light. To reduce any sort of problems in analysing the device further, such as unwanted vibration in the  $X_3$  coordinate, the same frame should be as rigid as possible and relatively 'easy' for manufacture. As such 3mm 6070 plate aluminium was chosen for the frame material. Extra care was taken into considering future modifications within the project, including mounting screws for possible

breaking systems or inclusion of other sensors, actuators or flywheel geometries and including other manufacturing techniques such as 3d printing. The one degree of freedom functional prototype should also be close to the final geometry for inclusion to be built in future projects such as an expansion to a full 3 degree of freedom, 3d pendulum.

To design the flywheel itself some initial constraints needed to be reasoned.

- Ideally low motor revolutions
- Easily manufacturable to reduce rotor unbalance
- Low rotational resistance (low moment of inertia)

Going under a basic assumption the entire device when fully assembled would have an approximate mass of 1-200 grams with a potential energy of  $V_p$  the opposing required kinetic energy  $T_p$  of the flywheel was calculated with the following assumptions  $E \stackrel{!}{=} 0 \Leftrightarrow V = -T$  where  $\dot{\varphi}$  will be functionally low with  $\dot{\varphi} \leq 2\pi \frac{\text{rad}}{\text{s}}$  when stabilised.

Solving the maximum potential energy of the system at  $V_p = 9.81 \frac{m}{s^2} \times 0.15 \text{ kg} \times 0.09 \text{ m} = 0.132435 \text{ J}$  the total energy that must be removed from the system when at the unstable equilibrium due to disturbances is relatively low. When considering the energy of the flywheel itself from equation 1.8 rewritten here

$$T_p = \frac{1}{2} \Theta \omega^2$$

The total energy of the flywheel seen in Figure 2.2 is linearly dependent on the moment of inertia and quadratically dependent on the angular velocity, as the total required energy to counterbalance the potential energy  $V_p$  is small, and the EC45 flat having a large total RPM range, calculating an exact moment of inertia is not required beyond keeping the geometry as uncomplicated as possible, balanced and below the load limits of the motor. However, as manufacturing tolerances and wheel unbalance cannot be easily predicted, high angular velocities are still unwanted as they may bring in instabilities, though these may not present themselves until the highest speeds, some care must be taken in providing a 'high enough' inertia so that high velocities aren't required but a simple flywheel form so unbalance and tolerance failures don't destabilise the system.

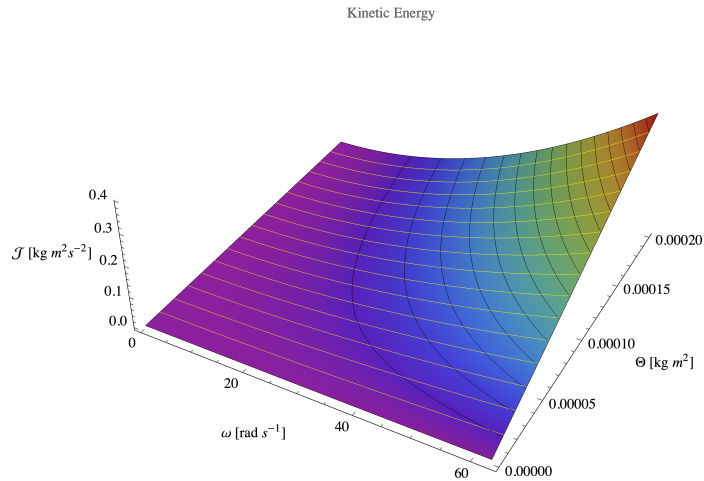


Figure 2.2: Kinetic Energy plotted against flywheel angular velocity and moment of inertia. Changes in Moment of Inertia have negligible changes in Energy.

# Chapter 3

## Parameter Identification

What one man can invent another can discover.

---

Sherlock Holmes

Much to the surprise of some individuals, even those formally educated in design, often times things simply don't work as planned.[17] Small discrepancies in design tolerances or unexpected heterogeneity of parts or completely unknown physical phenomenon can present themselves in the least expected manner, leading to instability or, in the worst case, to catastrophic failure.

Such an example of this can be found when reflecting back on the space programs during the Cold War era. The "Pogo effect" was described as "...a low frequency oscillation in the combustion chamber, or propellant feed system, excites the longitudinal vibration mode of the entire rocket vehicle." This caused rockets to quite literally jump like a Pogo stick mid-flight. This particular unexpected problem was such an issue that virtually none of the Soviet N-1 rockets had a successful launch. [18]

Although rockets can be reduced down to marginally expensive, albeit fancy, flying pendulums they are extremely complex in design which carries an unsurprising amount of unpredictable unknowns. The *fly* pendulum is in contrast not quite as fancy or as expensive: it, like the rocket, is unstable when trying to counteract gravity and its parameters must still be fully identified. Without proper identification of the systems parameters it will surely be doomed to failure.

### 3.1 Parameters to identify

In order to fully design a controller for the F.P. numeric definitive values must be found. When reflecting back on the original equations of motions 1.26

$$\Theta\ddot{\alpha} + j_w\ddot{\varphi} + r_b\dot{\alpha} + g(km_w + lm_b)\sin\alpha = f(t) \quad (3.1)$$

and

$$j_w(\ddot{\alpha} + \ddot{\varphi}) + r_w\dot{\varphi} = \tau u(t) \quad (3.2)$$

Some parameters such as pendulum masses  $m_b$ ,  $m_w$  can be directly measured with a scale or are immediately chosen in the design criterium such as  $k$  and  $\tau$ . The parameters to be determined are the rest, including  $\Theta, j_w, j_b, r_b, r_w$  and centre of mass  $l$ . These parameters beyond the centre of mass cannot be directly measured and must be indirectly calculated using the available IMU sensors and the properties of the system dynamics.

### 3.2 IMU Calibration

Before the motion processing unit can be used for calculating system orientation they first must be calibrated. Although these sensors are factory calibrated, due to small heat induced stresses and

misalignments from soldering and mechanical mounting there will be small errors in the sensor results.

### 3.2.1 Accelerometer and Gyroscope

The FXOS8700 can provide either direct axis dependent accelerations or in the 'raw' 12bit format. To get a more accurate result of each  $a_i$  the mean of 2000 values of each axis were first recorded when each sensor axis was placed parallel to gravity and stabilised providing  $\bar{a}_i$  means as seen in Figure 3.1

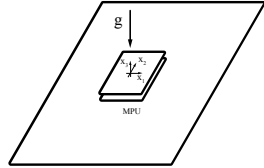


Figure 3.1: Accelerometer calibration technique

Once this was found the standard deviation of the measurements were taken where  $s_i = \sqrt{\frac{1}{n-1} \sum_{j=1}^n (\bar{a} - a_{ij})^2}$  and calculated for each axis, providing  $s_i$  values. Once these were found, an algorithm

$$a_i(a_{raw}) = \bar{a}_i \times \frac{a_{raw}}{4096} - s_i \quad (3.3)$$

was programmed to calculate corrected acceleration values for each axis. The selected gyroscope sensor already provides exceptional characteristics against gyroscopic drift requiring no further adjustment or compensation values.

### 3.2.2 Magnetometer

The magnetometer of the IMU is required for further use in the calculation of orientation.[19] It is used to help calculate the absolute position of the sensor using the earth's magnetic fields and as such is the most sensitive and likely initially inaccurate sensor. Its calibrations require finding hard- and soft-iron offsets. The magnetometer, combined on the same breakout board as the gyroscope and accelerometer is near the BLDC motor and its global location likely different than its original manufacture, therefore it must also be calibrated. To find these offset values the software MotionCal developed by Paul Stoffregen of PJRC was used to find the offset values and programmed into the controller firmware.

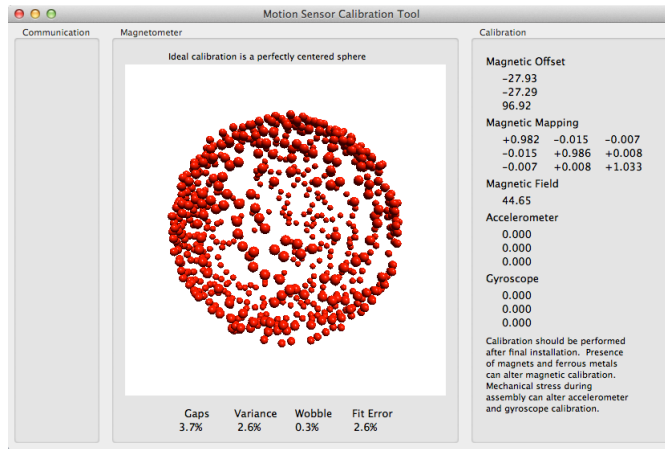


Figure 3.2: MotionCal from Paul Stoffregen, PJRC

### 3.3 Madgwick Filter

To find the absolute orientation of the F.P. the direct 'raw' sensor results are less than helpful by themselves. Required inputs for the Flywheel pendulum include angular velocity  $\dot{\alpha}$  which can be read directly from the gyroscope, flywheel angular velocity  $\dot{\phi}$  which will be read directly from the servo controller. Leaving the absolute angle  $\alpha$  to be calculated and derived. This value can be calculated in many ways including the simple integration of the directly measured  $\dot{\alpha}$ . This however is extremely dependent on the discretised sensor values and noise, which may lead to large spikes and instability, adding any filters to smooth the gyroscope data and then integrating may cause significant phase lag if poorly designed and not accurately represent the system at any given moment. An example of this can be considered when looking at a noisy signal sample

$$\dot{\alpha}(t) = e^{-t} \delta(t) \left( \sin(\omega t) + \frac{1}{6} \sin(20\omega t) \right)$$

Applying a second order Butterworth lowpass filter and then integrating results in a signal that not only has massive phase lag, but also displays oscillation due to the multiple complex pair poles of the filter as seen in Figure 3.3

To avoid such problems there have been multiple implementations of different "fusion" algorithms including the 'Kalman filter', and 'Complimentary Filter'. Both of these and others have been in frequent use in many industries including aerodynamics, robotics, navigation and other motion analysis. [19] The Madgwick filter is one of such fusion algorithms, combining MARG sensor arrays (all axis degree of freedom signals,  $a_i, g_i$  and  $m_i$ ) and outputting the results in absolute orientation. With accurate results compared to other commercial or long standing used filters, the madgwick filter can run on low power processing devices is fast with little phase lag. [19]

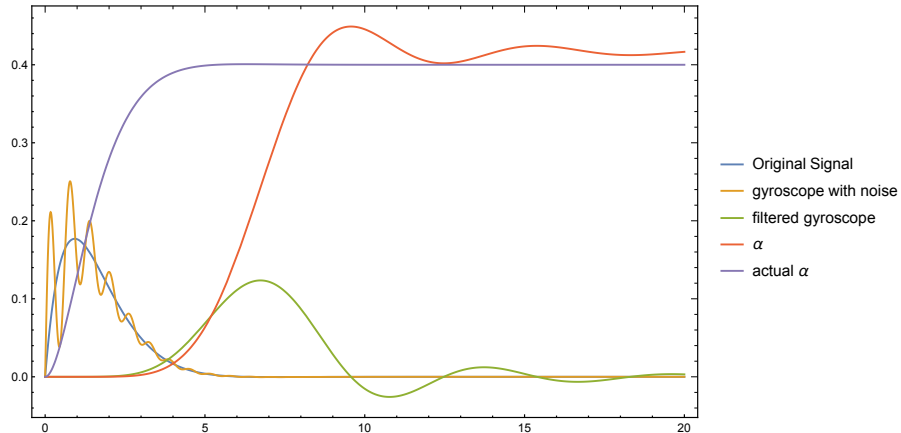


Figure 3.3: Signal Lag

### 3.4 Centre of Mass Approximation

To find the length of the F.P. centre of mass vector  $\underline{r}$  simple geometric analysis of the pendulum body and the effects of gravity can be applied. The centre of mass of the pendulum body will always lay on the same orthogonal line perpendicular to the base floor. Knowing this affect, the deflection of the body while hanging can be directly measured.

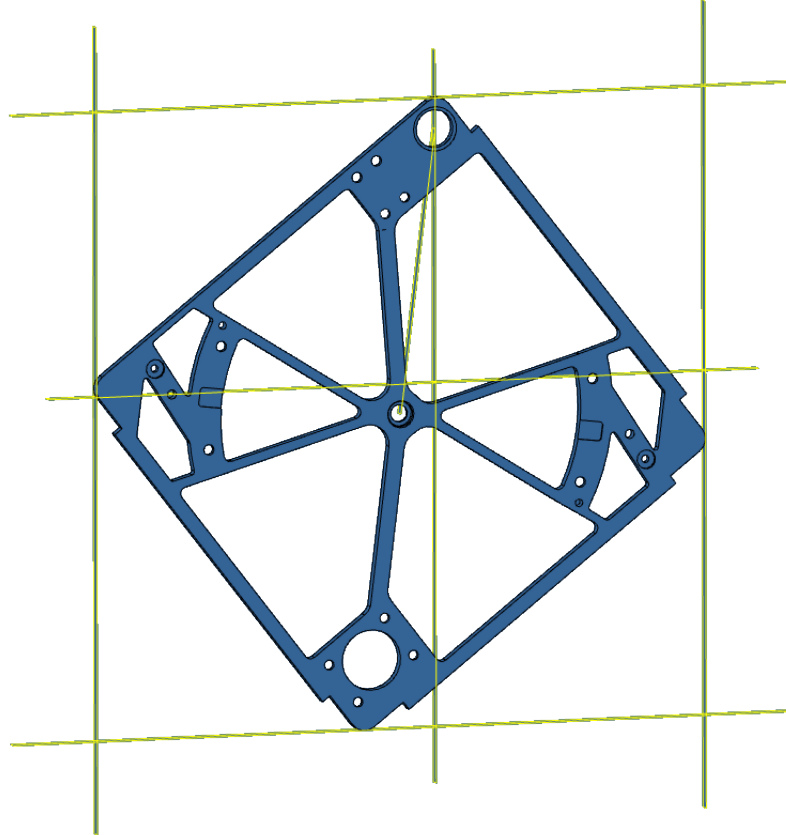


Figure 3.4: Geometric analysis

With the outer boundary planes in place and measured, the body need only be rotated once to a 90 degrees separated point from the pendulums rotational axis, measured and plotted again. This new plane which crosses the first will thus give an approximate centre of mass dimension barring measurement tolerances. The approximate measurement of 0.079886[m] was found following the assumption that the centre of mass will be below the motors mounting point. This is due mechanical mounting, and sensor and motor cables.

With little more than a measuring tape, a right angle edge and some intuition a very accurate approximation of a bodies centre of mass can be easily found.

## 3.5 This one goes up to 11

### 3.5.1 Nonlinear Identification

As seen in the previous subsections the parameter of a system can be quickly and accurately calculated when using some intelligent tactics and assumptions. However the linearisation of a nonlinear system is only good for a particular working point. [11] If the system wonders too far away from this particular operating point, the systems solution can be drastically incorrect and completely useless.

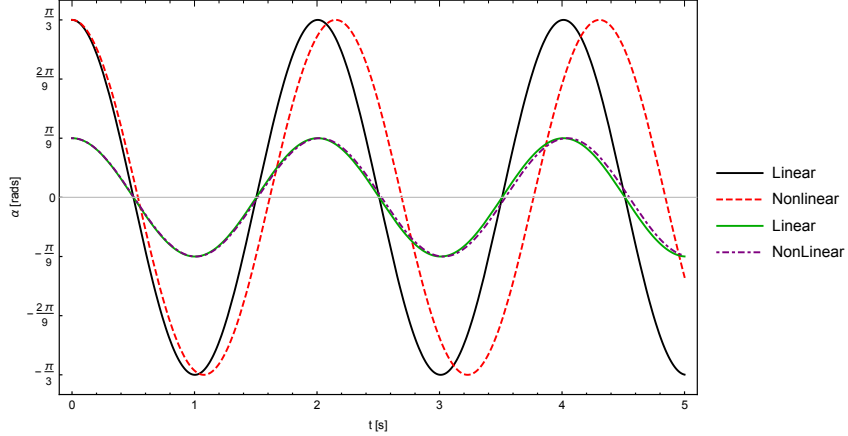


Figure 3.5: Comparison of error between small displacement versus larger.

Considering the the oscillation of the pendulum in Figure 3.5, when linearising around the operating point  $\frac{\pi}{9}$  the progression of the amplitude and oscillations stay nearly uniform with very marginal divergence. However by increasing the initial conditions to  $\frac{\pi}{3}$  and linearising, the aberration of the oscillation is already visible before even the first half period. While in general the error of margin is small enough for many systems, for some values, particularly those such as friction or inertia, parameters that can cause drastic instability when incorrectly calculated, other techniques must be applied to get accurate approximations.

### 3.5.2 Flywheel Moment of Inertia, Friction Coefficient

Equation 3.2 describes the dynamics of the flywheel and motor. When setting  $\alpha = 0$  equation 3.2 becomes

$$j_w \ddot{\varphi} + r_b \dot{\varphi} = \tau u[t] \quad (3.4)$$

Where the sum of moment of inertia times the angular acceleration is the result of acting torques, the basic electric motor equation will suffice for the control of the flywheel pendulum. Recall the EC45 Flat, or specifically the servo controller the Escon 24/2 has an internal PI current controller, running at 10khz, the motor, although in reality not a common DC motor, but rather a permanent magnet synchronous motor with different dynamics to be considered and controlled via a PWM signal, the motor itself can be considered continuous where the error of ignoring the escons PI dynamics and discretised control signal is insignificant compared to the simplicity given of the general electric motor equation and a continuous dynamic.

Equation 3.4 is a LTI ODE allowing one to solve readily with common techniques, include Laplace. When solving this will give a direct analytical solution of  $\varphi(t)$ . However the motor angle evolution for the control scheme is unimportant, and less so for the identification of the total inertia and friction parameters. Solving the ODE with initial conditions  $\varphi(0) = u_0$  and  $\dot{\varphi}(0) = \omega$

$$\varphi(t) = \frac{j_w e^{-\frac{r_w t}{j_w}} (\tau u - \omega_0 r_w) + \omega_0 j_w r_w - \tau u j_w + t \tau u r_w + u_0 r_w^2}{r_w^2} \quad (3.5)$$

and differentiating once provides the drastically reduced equation

$$\dot{\varphi}(t) = \frac{e^{-\frac{r_w t}{j_w}} (\omega_0 r_w - \tau u_0) + \tau u_0}{r_w} \quad (3.6)$$

Assuming initial conditions are  $\dot{\varphi}(t = 0) = \omega_0 = 0$  gives the final equation.

$$\dot{\varphi}(t) = \frac{\tau u_0}{r_w} \left( 1 - e^{-\frac{r_w t}{j_w}} \right) \quad (3.7)$$

Equation 3.7 is a typical decaying exponential response to a given input. What is particularly difficult with this equation is that both the friction and inertia values appear in the solution as a ratio to one another. Meaning there is any infinite combination of value pairs that could provide a valid fitting. Trying to linearise this function around the operating point of the stationary system,  $\omega_0 = 0$  gives

$$\dot{\varphi}(t) \approx \frac{\tau u_0 t}{J_w} \quad (3.8)$$

As a result. When comparing the velocity evolution of both equations, it is immediately clear that the linearised function simply isn't up to the task for fitting of both parameters  $r_w$  and  $J_w$

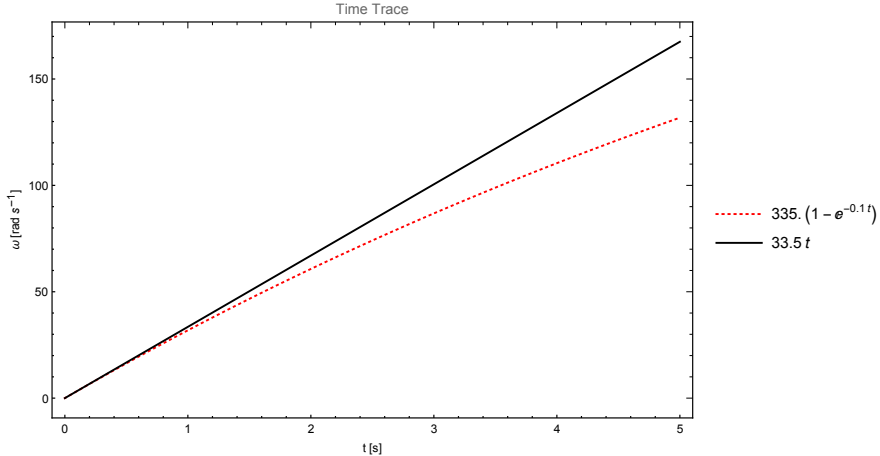


Figure 3.6: Time Trace of nonlinear and linearised function response

Given that the linearised function is only valid for an extremely small time period and only one specific input and that friction is completely missing from the equation, the original equation 3.4 will be used as the model for two nonlinear model fitting algorithms. Building a manual software interface, a manipulator was designed so that likely candidates of the parameters  $r_w$  and  $j_w$  could be found qualitatively.

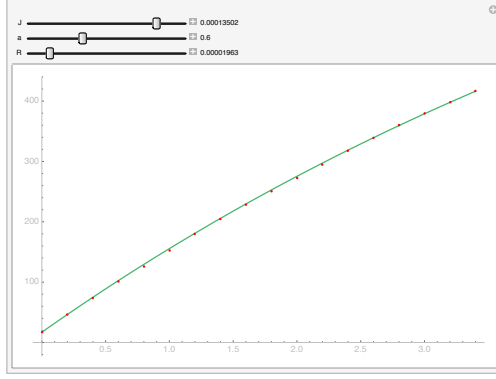


Figure 3.7: Parametric Nonlinear Mode Fitting interface manipulator.

With the new found initial values for a nonlinear model fitting function using nonlinear Gradient Methods an algorithm was written within the Wolfram Language® using the initial qualitatively found candidates  $r_0$  and  $j_0$  to calculate best fit parameters. Testing the motor at different current inputs ranging from 0-1[A] and calculating the mean, final 'best-fit' values were calculated to be:

$$r_w \rightarrow 0.0000175204, j_w \rightarrow 0.000136125 [kgm^2]$$

Providing another 2 identified parameters, leaving  $\Theta$ ,  $r_b$  left to solve.

### 3.5.3 Fullbody Moment of Inertia, Friction Coefficient

Recalling equation 3.1 and setting  $\varphi = 0$  and  $f(t) = 0$  the equation can be reduced to the compound pendulum equation:

$$\Theta\ddot{\alpha} + r_b\dot{\alpha} + g(km_w + lm_b)\sin\alpha = 0 \quad (3.9)$$

Providing the nonlinear model for identification of  $\Theta, \mu, r_b$ . A manipulator was designed, like the flywheel fitting, to find initial candidates to be used later in the automated fitting algorithm. This attempt was however halted due to a particularly large missing factor. When looking at the initial time trace, it has become apparent that the description of viscous friction  $F(\dot{\varphi}) = r_b\dot{\varphi}$  as described by the Rayleigh function 1.25 is unable to completely describe the effects of friction on the pendulum in small displacements.

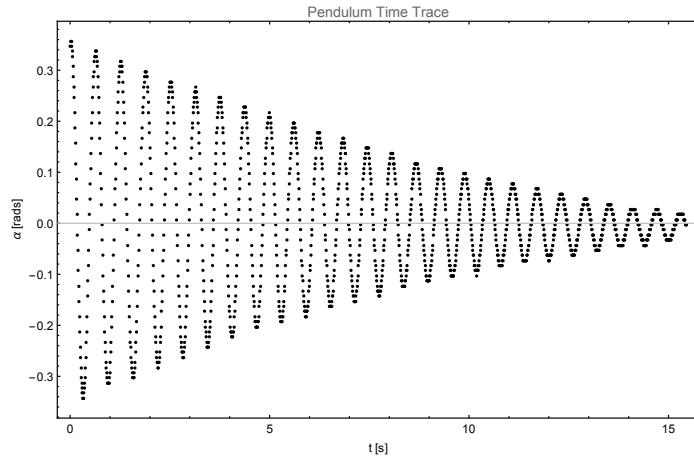


Figure 3.8: Time trace of the pendulum displaying nonlinear friction effects for low displacements  $\alpha \leq 0.1$

When looking at the solution to the basic LTI ODE equation  $\ddot{x} + 2D\omega_0 \dot{x} + \omega^2 x[t] = 0$  The resulting solution is a multiplicative exponentially decaying oscillating function  $c e^{-\omega_d t} \sin(at)$ . Due to the nature of the exponential function  $e^{-\omega_d t}$  the result can never approach zero as  $t$  approaches infinity. This is

clearly not the case for the real physical pendulum, as the system most certainly comes to a full stop at it's equilibrium.

Because of this the system equation must be expanded to compensate the new friction phenomenon. Taking the original function  $F(\dot{\varphi}) = r_b \dot{\varphi}$  and adding the the most basic form of the coloumbe friction  $F_c(\dot{\varphi}) = \mu \operatorname{sign}(\dot{\varphi})$  [20]. The system of equations can be redefined as:

$$\begin{aligned} \Theta \ddot{\alpha} + j_w \ddot{\varphi} + r_b \dot{\alpha} + \mu \tanh\left(\frac{\dot{\alpha}}{\iota}\right) + g(km_w + lm_b) \sin \alpha &= f(t) \\ j_w (\ddot{\alpha} + \ddot{\varphi}) + r_w \dot{\varphi} &= \tau u(t) \end{aligned} \quad (3.10)$$

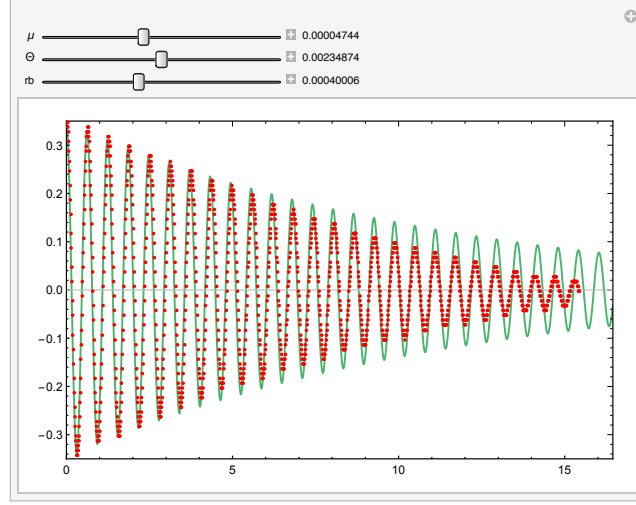


Figure 3.9: Parametric Nonlinear Model interface manipulator.

Due to the difficulty with numerical software when dealing with the  $\operatorname{sign}()$  function, this has been replaced with the  $\iota$  scaled  $\tanh(\frac{x}{\iota})$  function, providing a smooth approximation of  $\operatorname{sign}()$ . With a slightly more accurate friction model, the manipulator function was updated to include the new values  $\Theta$ ,  $\mu$ , and  $r_b$ . Allowing like the flywheel a qualitative candidate to be found. Using these values and applying to a nonlinear gradient algorithm the last parameters of the system of equations 3.10 have been fully identified as  $\Theta \rightarrow 0.0025925[\frac{kg}{m}]$ ,  $\mu \rightarrow 0.0004485$ ,  $rb \rightarrow 0.0000212$

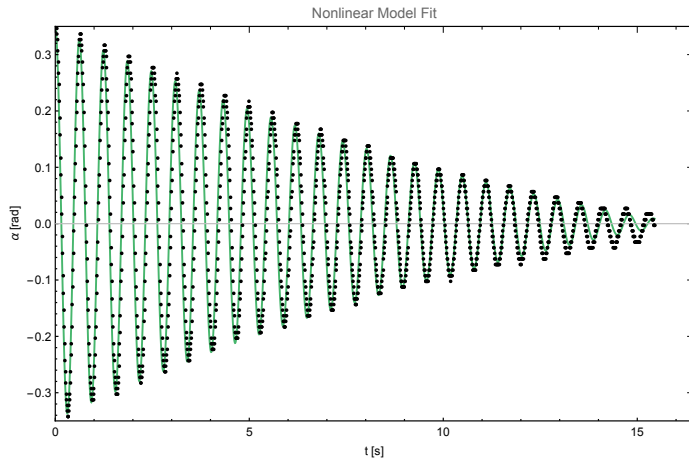


Figure 3.10: An overlay of the final fit function  $\alpha(t)$  over the time trace. A direct crossover from what appears to be viscous to a combination of viscous and columbe friction appears at  $t \approx 10s$

## 3.6 Conclusion

Parameter identification of any mechanical system is paramount to its understanding. Even with indepth knowledge of each part, their sum is very much more than their parts together. Although linear tools and analytics can be applied directly to some systems, using general approximations may end providing incorrect values that are acceptable for some, but completely disastrous for others.

Within this chapter the application of nonlinear tools have been applied to find better approximations of the system and confrontation of missing model dynamics bring up the evidence that all models are only as correct as the knowledge that can be attained by them. As one gets further into the development of a system and particularly its near exact physical identification it is paramount to be aware that the initial model itself may be wrong, and is certainly subject to change.

# Chapter 4

## Controller Design

This is a story about control, My control.  
Control of what I say, Control of what I do,  
And this time, I'm gonna do it my way, I  
hope you enjoy this as much as I do  
Are we ready? I am

---

Janet Jackson

The art of control is a suspicious one. Its definition - "to exercise authoritative or dominating influence" - is intimidating at best. But the direct influence of the universe around us has made the cold, warm with little more than dominating fire. Through simple 'control' of water flows humanity has bent the will of water for its own gain, creating at its simplest irrigation for early humanity's farming systems, to the Romans now famous plumbing and latrines all the way to powering turbines for electricity production.

With the use of control, systems that have been poorly designed can often be corrected. The motorised crane serves as a particularly good example. Without control, moving with (not necessarily) massive objects and abruptly stopping can cause massive unwanted swinging movements of said object, causing damage to surroundings, persons or the crane itself. Inherently unstable systems can be coerced into rejecting their normal stance and stand against gravity such as Kapitza's pendulum. [21] Controlling techniques and their applications on the systems around us are here to stay, as technologies become more specialised, faster and more powerful, the less they are within the grasps of any one (or millions of) human(s) to handle. Before their complications get the best of society, newer and better techniques must be learned, lest the controlled become the controllers.

### 4.1 Back to Basics: Part *Deux*

The Flywheel pendulum as a mechanical test bench is made inverted through the clever use of torque exchange. When considering the exchange of energy within the system, there is a storage within the potential energy and the kinetic energy, the total energy of the system remains constant (when neglecting dissipations) allowing the clever use of adding or taking away energy with the angular acceleration of a motor and a flywheel. Recall from equation 3.4 that the sum of total system torque is equal to the addition of motor input and frictional torque. It is coupled mechanically to the pendulum's body allowing for torque disturbances to be compensated for. Looking at a simplified free body analysis of the pendulum excluding dissipation forces in figure 4.1:

$$\sum_i^n M_a = F(t) l \sin(\alpha) + mgl \sin(\alpha) + \tau u(t) = 0 \quad (4.1)$$

and replacing  $\tau u(t)$  with equation 3.4 equivalency:

$$M_a = -j_w(\ddot{\varphi} + \ddot{\alpha}) = F(t) l \sin(\alpha) + mgl \sin(\alpha) \quad (4.2)$$

Implies that the total input of disturbances  $f(t)$  and gravity can be equalised with the input of input of the motor, or more specifically the negative acceleration of the flywheel. Through the physical

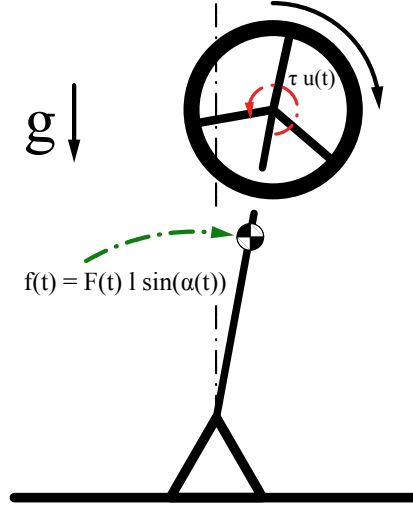


Figure 4.1: Torque exchange of the flywheel pendulum

coupling, an opposite opposing torque is applied, dissipating the input force and keeping the flywheel pendulum inverted.

#### 4.1.1 Analysis

During the identification of system parameters the system model of equations had to be updated to account for an expanded friction model. This must also be updated with the state space model 1.29.

$$\left( \begin{array}{c|ccc|c} & & & & \text{S} \\ \hline x_1 & 0 & 1 & 0 & 0 \\ x_2 & \frac{g(km_w + lm_w)}{\Theta + j_w} & -\frac{\mu + \iota r_b}{\iota j_w} & -\frac{r_w}{\Theta + j_w} & \frac{\tau}{\Theta + j_w} \\ x_3 & -\frac{g(km_w + lm_w)}{\Theta + j_w} & \frac{\mu + \iota r_b}{\Theta - j_w} & -\frac{\Theta r_w}{j_w^2 + \Theta j_w} & \frac{\Theta \tau}{j_w^2 + \Theta j_w} \\ \hline x_1 & 1 & 0 & 0 & 0 \\ x_2 & 0 & 1 & 0 & 0 \\ x_3 & 0 & 0 & 1 & 0 \end{array} \right) \quad (4.3)$$

and substituting all parameter values:

$$\left( \begin{array}{c|ccc|c} & & & & \text{S} \\ \hline x_1 & 0 & 1 & 0 & 0 \\ x_2 & 113.116 & -2.45364 & 0.00808392 & -15.4569 \\ x_3 & -113.116 & 2.45364 & -0.136792 & 261.555 \\ \hline x_1 & 1 & 0 & 0 & 0 \\ x_2 & 0 & 1 & 0 & 0 \\ x_3 & 0 & 0 & 1 & 0 \end{array} \right) \quad (4.4)$$

Extracting the system matrices  $\underline{\underline{A}}$ ,  $\underline{\underline{B}}$  and  $\underline{\underline{C}}$  initial inspection of the control system can be done. As the flywheel pendulum is a MIMO system, common pole and zero inspection of the transfer function cannot be easily applied. However, the eigenvalues of the  $\det(\underline{\underline{A}} - \lambda \underline{\underline{I}}^{3x3}) = 0$  will produce the poles of the system discovering if the system is stable. [22]

$$\det(\underline{\underline{A}} - \lambda \underline{\underline{I}}^{3x3}) = 0 = -\lambda^3 + q_1 \lambda^2 + q_2 \lambda + q_3 \quad (4.5)$$

Providing 2 negative and one positive poles on the real axis depicted in figure 4.2. The system is linearised around the operating point  $\pi$  and is in its unstable equilibrium, meaning it is in this state neither stable as seen by the positive pole nor is it oscillating due to lack of imaginary eigenvalues.

Further using the Kalman Rank criterium, the observability and controllability of the pendulum can be determined. The observability matrix  $\underline{\underline{S}_o}$  and controllability matrix  $\underline{\underline{S}_c}$  with the Kalman criterium

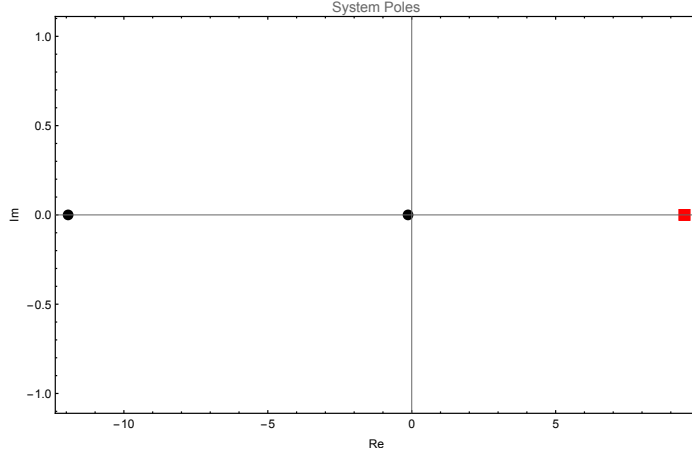


Figure 4.2: System Eigenvalues

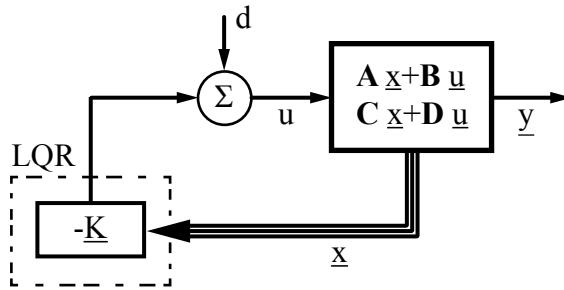
state that when these matrices have full Rank, then the system is respectively fully observable and fully controllable.[23] Defined as:

$$S_o = \begin{pmatrix} B & AB & \dots & A^{n-1}B \end{pmatrix}, S_c = \begin{pmatrix} C \\ AC \\ \vdots \\ A^{n-1}C \end{pmatrix}$$

Both  $S_o$  and  $S_c$  have full rank of 3 when calculated. With the analysis of the system fully discovered, a full statefeedback controller can be chosen and developed.

## 4.2 Linear Quadratic Regulator

Knowing that the pendulum is fully observable, which wasn't specifically new information, (being that the sensors discussed in chapter 3 were used to measure all states anyways...) the pendulum will be controlled via the optimal "Linear Quadratic Regulator" state feedback controller. Seen in figure 4.3. This controller one of the most common optimal control problems and can be used to optimise a quadratic cost function on the system controller gains  $K_i$ . [22]

Figure 4.3: Linear Quadratic Regulator with  $\underline{K}$  gains, additive  $d$  disturbances and State Space Model Block  $\dot{x}$ ,  $y$ 

A common known technique to control the state space system is "Pole Placement". Where the characteristic polynomial  $P(s)$  of the closed loop statespace system is  $\dot{\underline{x}} = (\underline{A} - \underline{B} \underline{K}) \underline{x}$  ideal poles can be chosen by the designer and the polynomial solved to find the appropriate  $\underline{K}$  gains[22]. The Linear Quadratic Regulator on the other is an alternative solution to the full state feedback controller problem.

Given a multi-input statespace system an attempt to minimise the infinite horizon function  $J$ :

$$\hat{J} = \int_0^\infty (x^T \underline{\underline{q}} + u^T \underline{\underline{r}} u) dt \quad (4.6)$$

The equation  $\hat{J}$  with symmetric, and in this case, diagonalised positive (semi-)definite weighting matrices  $\underline{\underline{q}}$  and  $\underline{\underline{r}}$ . The function is a balance of the distance from state initial conditions (the origin) and the quadratic cost of controller input. With well designed weighting matrices the cost of motor input and rate of convergence of the system to the origin point  $x_0$  can be balanced against each other in order to calculate the most optimal gains. [22]

Choosing diagonalised  $\underline{\underline{q}}$  and  $\underline{\underline{r}}$  weighting matrices allows the 'feelings' or experiential intuition of the designer to be applied to each state variable. As there are no particular heuristic methods such as those of Nicolas Ziegler to apply, simulation and testing are the only appropriate methods for finding ideal weightings. Each element of the matrix is effectively applied as the weighting value of each feedback state variables, the solution to the LQR equation is a linear control law:

$$u = -\underline{\underline{Q}}^{-1} \underline{\underline{B}}^T \underline{\underline{P}} \quad (4.7)$$

Matrix  $\underline{\underline{P}}$  is positive definite symmetric and element of  $\mathbb{R}^{nxn}$  which satisfies the *algebraic Riccati equation* [22]. Should a solution exist, a closed loop stable system will have been created.

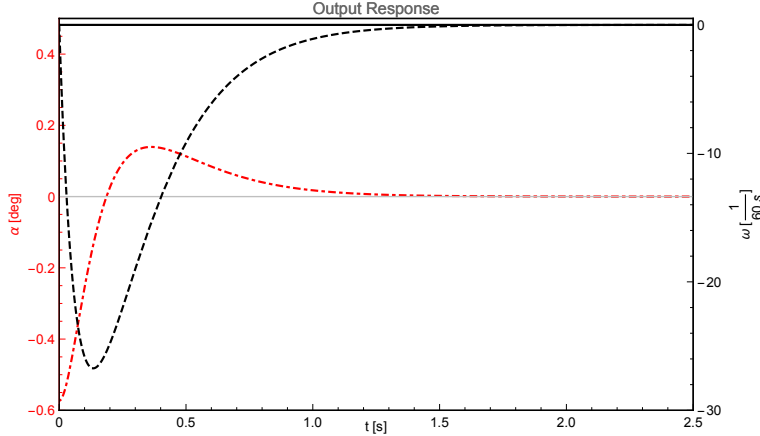


Figure 4.4: The ideal simulated Output response tracking around initial operating point  $\pi$

Using Wolfram Language® a function was designed to solve the optimal gains, with solution  $\underline{\underline{K}}^T$  as the final calculated gain values. Starting with the simple identity matrix  $\underline{\underline{I}}^{3x3}$  and increasing  $q_i$  weighting then simulating with the numerical software Mathematica® a satisfactory transient response of the pendulum was found.

$$\underline{\underline{r}}^{-1} \cdot \left( \underline{\underline{B}}^T \cdot \text{RiccatiSolve}[\{\underline{\underline{A}}, \underline{\underline{B}}\}, \{\underline{\underline{q}}, \underline{\underline{r}}, \underline{\underline{P}}\}] + \underline{\underline{P}}^T \right) = \underline{\underline{K}}^T = (-24.4786, -2.14922, -0.0228898) \quad (4.8)$$

After finding the system gains, the feedback statespace model was calculated and simulated against disturbance rejection of forces  $f(t) = a e^{b(t-t_i)^2}$ .

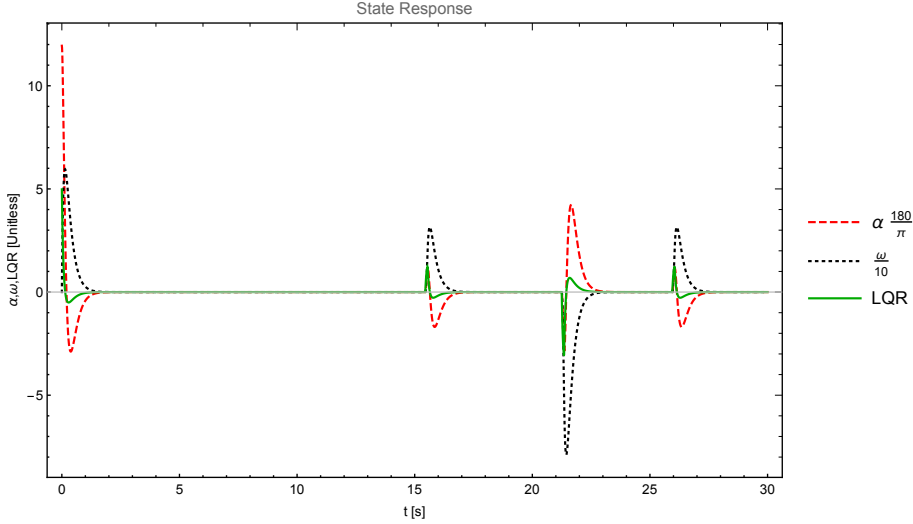


Figure 4.5: Simulated State response to disturbance rejection.

The system settles within 1[s] with minimal reactionary displacement, quick return and low motor effort. Although it seemed apparent the weighting values should be highest for the state variable  $\alpha$ , meaning the LQ regulator should bring at all costs the pendulum back to the initial condition  $\pi$  the system was never stable due to extreme overshoots from abrupt motor breaking. This was due to misunderstandings of the LQR mathematical properties and calculated gain results. The gains provided assume infinite effort on the controller and absolutely exact state values can be provided, which in reality certainly cannot be produced. After a certain amount of experimentation it was found weighting needed to be most carefully applied to the angular velocity  $\dot{\alpha}$  of the pendulum body, as the device should return to initial conditions  $\alpha = 0$  slowly but may overshoot somewhat rather than instantly stopping all acceleration the moment the initial state  $\pi$  has been reached.

#### 4.2.1 Conclusion

With careful analysis of system properties different control strategies can be easily applied and quickly simulated. The development of a basic regulator with numerical softwares can be quick and relatively painless. However it is important to know that easily run scripts do not equate with nor replace the intuition of an experienced designer. The application of any particular control scheme must be weighed with system underpinnings and dynamics in mind. Ignorant understanding of the system, or the controller itself, and haphazard application of mathematical scripts will only provide failure and frustrations to the designer. Without proper dominion of the system, they themselves will surely fall into a spiral of uncontrolled madness.

# Chapter 5

## Implementation and Results

To understand the best is to work on it's implementation

---

Jean-Marie Guyau

Typical to many engineering projects, or any project in general, the conception, designing and identification of any particular system, however arduous and unending it may seem, eventually does come to an end. The theories fully applied and simulated giving perfect results and inspiration to finish the final step generally fail to show the oncoming difficulties when it comes to actually *implmenting* them. It is worth considering the 90/90 rule coined by Tom Cargill:

The first 90 percent of the code accounts for the first 90 percent of the development time.  
The remaining 10 percent of the code accounts for the other 90 percent of the development time.

It can be assumed that there is a pinch of truth in the assumption that the programming and implementation of any giving programming project is not going to be trivial, this was certainly the case when programming the flywheel and the controller scheme. Using the Wiring language the Huzzah esp32 microcontroller was programmed following typical Arduino style syntax and methodology. Using this language common sensor libraries the code for the flywheel pendulum is as generically written as possible, where the use of the 'package' can be applied to any number of Arduino compatible microcontrollers with minimal change in code.

The feedback controller was generated using the *MicrocontrollerKit* of the Wolfram language ®, this was generated with a 1 [ms] sample rate, allowing for the system oscillation, which is approximately 1.5hz, to more than adequately be sampled following the Nyquist rate criterium of sample rate being a minimum of twice as fast as the physical process. Ensuring the exclusion of system instability through the discretised signal replication. [24]

## 5.1 Results and Comparison

Taking a time trace of the pendulum seen in figure 5.1 with an initial displacement of  $\alpha_0$  the system was allowed to selfstabilize. Timing for 30 seconds and injecting a disturbance at regular intervals and testing the rejection response, the flywheel pendulum was able to reject large disturbance forces and displacements up to nearly  $\pm 15$  degrees. The controller effort is near continuous zero and what appears to be a steady state error in the motor angular velocity, likely attributed to numerical error accumulation and small system measurement noises.

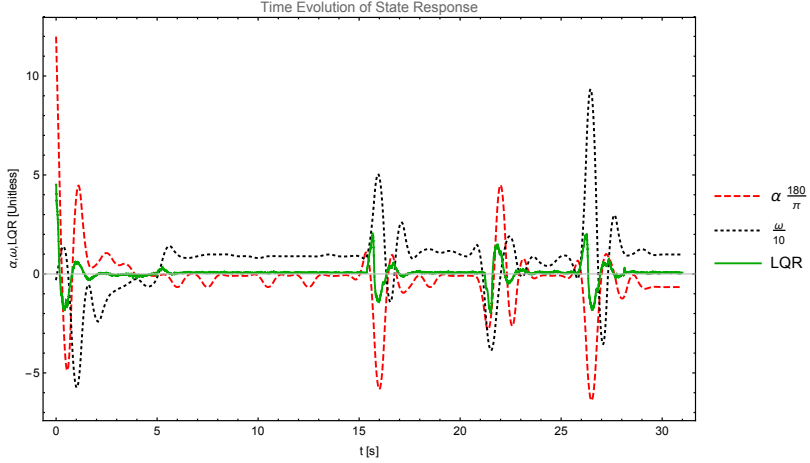


Figure 5.1: Time trace of Controller and StateSpace Response to disturbances at  $t_i$  times.

A comparison of the time trace with a simulation in figure 5.2 shows that the modelling and controller dynamics reproduce the dynamics of the theoretical model relatively closely. The response of the pendulum angle evolution is somewhat different than in the simulation, with always one more oscillation beyond the zero axes before returning to the tracking angle. This is likely due to the steady state error that the controller must correct for first as there is already energy within the system to be dissipated.

Curiously the system is still able to stay stable with smaller angle displacement, but much larger forces with recovery action (albeit much a much larger amplitudes) as seen at circa 26[s]. This effect is easily understood through the much larger system motor angular velocity, the force was dissipated through the increase in flywheel momentum. Further study and optimisation of the controller gains can be investigated to further increase the robustness of the inverted pendulum and remove steady state error, these will be left for future study.

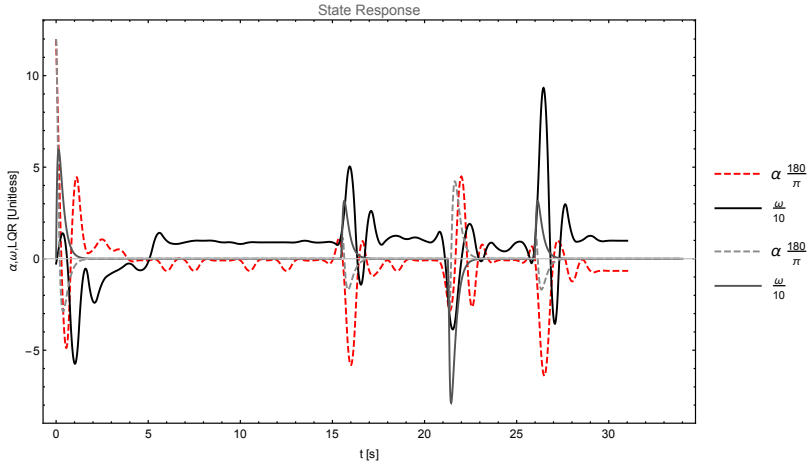


Figure 5.2: Comparison of system with Simulation

## 5.2 Conclusion and Future Work

The inverted pendulum is a classic among control problems: ideal for academic study with simple physical movement, yet surprisingly nonlinear and difficult to model dynamics. This lends itself for the development of experience and intuition in many disciplines of engineering, including mechanics, mathematics, electronics, programming and control. Although the system is basic, the dynamics and use of the pendulum surprisingly proves itself to be particularly interesting when considering robotic appendages or rockets. The inverted pendulum test bench was conceptualised as an instrument to be used in student experimentation internships, where safe use due to low voltages, machine power, size and simplicity can allow for direct teaching and application of motor drive related control theories and mathematical modelling. The use of open source hardware and software (excluding a few proprietary motors) allows for easy sharing and upgrading of the test bench.

The flywheel pendulum lqr control and parameter identification methodologies allow for use within other disciplines where system properties are far too difficult to regulate over a single measurement error value or nonlinearity affects the results of any common linearisation techniques too drastically to be useful. Further development of the pendulum can be easily shared through open platforms and included within larger more complicated projects. Future work will be conducted on realising a fully stabilised inverted 3d pendulum taking cues from the learned methods during this project.

Hopefully this particular project will provide inspiration to those looking to defy the typical and build their own automatons what the greeks could only dream of so long ago.

# Bibliography

- [1] Willie Scott. *History of Automated Assembly*. URL: <https://www.brighthubengineering.com/manufacturing-technology/126293-history-of-automation-in-manufacturing/>.
- [2] S Trymbaka Murthy. *Textbook of Elements of Mechanical Engineering*. 3rd ed. K International Publishing House, 2010. ISBN: 978-9380578576.
- [3] A.T. Murray (uebers.) *Illiad*. Hom. II. 18.360. Perseus, 762 BC.
- [4] Ian Bruce (uebers.) *Horologium Oscillatorium: sive de motu pendulorum ad horologia aptato demonstrationes geometricae*. 1st. Christian Huygens, 1673.
- [5] D.J. Acheson and T. Mullin. *Upside-down pendulums*. 366:215–216. Nature, 1993.
- [6] Mark W. Spong, Peter Corke, and Rogelio Lozano. “Nonlinear Control of the Inertia Wheel Pendulum”. In: *Automatica* 37 (1999), pp. 1845–1851.
- [7] Isaac Newton. *Philosophiae Naturalis Principia Mathematica*. 3rd. Christian Huygens, 1728.
- [8] Joseph-Louis Lagrange. *Mécanique Analytique*. Vol. 2. Cambridge Library Collection - Mathematics. Cambridge University Press, 2009. DOI: 10.1017/CBO9780511701795.
- [9] Eric W. Weisstein. *Euler-Lagrange Differential Equation*. 2020.
- [10] J. W. Strutt. “Some General Theorems relating to Vibrations”. In: *Proceedings of the London Mathematical Society* s1-4.1 (1871), pp. 357–368. DOI: 10.1112/plms/s1-4.1.357. eprint: <https://londmathsoc.onlinelibrary.wiley.com/doi/pdf/10.1112/plms/s1-4.1.357>. URL: <https://londmathsoc.onlinelibrary.wiley.com/doi/abs/10.1112/plms/s1-4.1.357>.
- [11] Taylor Brook. *Methodus Incrementorum Directa et Inversa*. Vol. 1. Cambridge University Press, 1715, pp. 21–23.
- [12] Keith Henry Sonja Alexander Lynn Jenner. *NASA Selects Top Inventions of the Year*. 1999.
- [13] Prof. Raffaello D’Andrea Michael Muehlebach. *Cubli*. 2011.
- [14] Adafruit. *IMU FXOS8700 Break Out Board*. 2020.
- [15] maxon motor ag. “EC 45 Flat”. In: *Reference documentation* (2017).
- [16] maxon motor ag. “ESCON Module 24/2”. In: *Reference documentation* (2014).
- [17] Unknown. *Citation Needed*.
- [18] Tom Irvine. “VIBRATION IN ROCKET VEHICLES DUE TO COMBUSTION INSTABILITY”. In: (2011).
- [19] Sebastian O.H. Madgwick. “An efficient orientation filter for inertial and inertial/magnetic sensor arrays”. In: (2010).
- [20] V. van Geffen. “A study of friction models and friction compensation”. In: (2009).
- [21] Kapitza P.L. “Dynamic stability of a pendulum when its point of suspension vibrates”. In: *Soviet Phys* (1951), pp. 588–597.
- [22] Richard M. Murray Karl Johan Astrom. *Feedback Systems*. 2nd ed. Princeton University Press, 2016.
- [23] Jan Lunze. *Regelungstechnik 2*. 9th ed. Springer Vieweg, 2016. DOI: 10.1007/978-3-662-52676-7.
- [24] Harry Nyquist. “Certain topics in telegraph transmission theory”. In: *Proc, IEEE* (1928), pp. 617–644.